Formation of the Ho/CdSe(10$\bar{1}$0) interface

S. L. Molodtsov,* M. Prietsch, C. Laubschat, and G. Kaindl
Institut für Experimentalphysik, Freie Universität Berlin, Arnimallee 14, D-14195 Berlin-Dahlem, Germany

A. V. Fedorov and V. K. Adamchuk
Institute of Physics, St. Petersburg State University, St. Petersburg 198904, Russia
(Received 23 November 1992; revised manuscript received 26 July 1993)

Auger-electron spectroscopy, Auger depth-profile analysis, as well as photoelectron spectroscopy give clear evidence for several stages in the formation of the Ho/CdSe(10$\bar{1}$0) interface. For Ho coverages lower than a critical thickness of $\simeq 1$ Å, no reaction or intermixing of the components was found. In the range of intermediate coverages, $2\,\text{Å} < \theta < 20$ Å, Ho-Se chemical reactions are observed leading to a release of Cd. For higher Ho coverages, $\theta \geq 20$ Å, this stage changes to a regime that is characterized by considerable Cd segregation and surface metallization. The presence of this metallic Cd layer prevents Ho diffusion and inhibits Ho-Se chemical reaction upon further deposition of Ho.

INTRODUCTION

The considerable interest in experimental and theoretical studies of metal/semiconductor interfaces in the recent past is certainly a consequence of the technological importance of these junctions.[1,2] Of particular interest for applications are diffusion phenomena and chemical reactions in the interfacial region, which have direct influence on the formation of Schottky barriers and on the macroscopic properties of metal/semiconductor junctions.

Up to now, mostly interfaces of Si, Ge, or related III-V compound semiconductors, in particular GaAs, with noble and transition metals have been investigated;[1,3,4] however, the interest in junctions with rare-earth (RE) metals is also growing.[5–12] With their comparably low work functions, the RE metals are promising candidates for Schottky-barrier formation. The high chemical reactivity of the RE metals allows the formation of stable compounds at the interfaces. Oxides of some RE metals or mixtures of them have been found to yield good-performance thin-film transistors or capacitors based on CdS and CdSe. Promising characteristics have also been found for semiconductor/insulator interfaces between ternary CdS_xSe_{1-x} semiconductors and RE oxides.[13]

We report here a detailed study of the reactive interface between Ho and CdSe(10$\bar{1}$0) by Cd 4*d* core-level and valence-band photoemission (PE), supplemented by detailed studies of the Se-*MVV*, Cd-*MNN*, and Ho-*NON* where Se denotes $M_{4,5}VV$, Cd denotes $M_{4,5}N_{4,5}N_{4,5}$, Ho denotes $N_{4,5}O_{2,3}N_{67}$, Auger-electron spectra (AES) as well as Auger depth-profile analysis. In this way information on the chemical structure of the Ho/CdSe interface was obtained and the magnitude of band bending (0.58 eV) for Ho coverages less than 0.2 Å was determined. In addition, we obtained evidence for the existence of a critical Ho coverage of $\theta_c \simeq 1$ Å for the beginning of Ho-Se chemical reaction and component interdiffusion. A similar behavior has been observed for some other reactive metal/semiconductor junctions.[14] For high Ho coverages, $20\,\text{Å} < \theta < 30$ Å, considerable enhancements of the element-specific PE and AES intensities from Cd are found, which can be explained by segregation of Cd to the surface as a consequence of chemical reaction between Ho and Se at the interface.

EXPERIMENTAL

Angle-resolved PE measurements were performed with a rotatable hemispherical analyzer (VSW-ARIES) with an acceptance angle of $\pm 2°$ using synchrotron radiation from the TGM-3 beamline at the Berliner Elektronenspeicherring für Synchrotronstrahlung (BESSY). The total-system resolution was $\simeq 0.25$ eV full width at half maximum, and the reproducibility of measured binding energies (BE's) is estimated to be ± 0.05 eV. All PE spectra were taken in normal-emission geometry. The recorded spectra were least-squares fitted with Lorentzian or Doniach-Sunjic line shapes convoluted by a Gaussian to account for finite experimental resolution. AES and AES-profile analysis data were obtained in a RIBER-LAS-3000 spectrometer with a resolution of 0.2% and a primary-electron energy of 3 keV. The base pressure in both experimental chambers was $\simeq 10^{-10}$ Torr.

CdSe(10$\bar{1}$0) *p*-doped wafers were cleaned by Ar^+ sputtering and annealed by electron bombardment from the back. These cleaning cycles were repeated until no traces of C or O could be detected in the AES or valence-band PE spectra, and sharp low-energy electron diffraction (LEED) patterns were obtained. After careful outgassing, Ho of 99.99% purity was evaporated from a tungsten coil and deposited onto the CdSe substrate at room temperature at a pressure of $\simeq 8 \times 10^{-10}$ Torr. The deposition rate was monitored by a quartz microbalance. Following each Ho-deposition step, Cd 4*d* core-level and valence-band PE or AES spectra were recorded. The AES-profile analysis of the Ho/CdSe interfaces for various Ho coverages was performed by alternating layer-by-layer Ar sputtering with grazing-incident Ar^+ ions of 1 keV energy, and AES employing the Se-*MVV*, Cd-*MNN*, and Ho-*NON* Auger signals.

RESULTS AND DISCUSSION

A. Cd 4*d* core-level and valence-band photoemission

Cd 4*d* core-level PE spectra, taken at 50 eV photon energy for various Ho coverages, are shown in Fig. 1(a) together with the results of least-squares fit analyses (solid lines through the data points and individual subspectra). The spectra have been normalized to constant height to emphasize changes in line shape. The Cd 4*d* PE spectrum from a freshly cleaned CdSe(10$\bar{1}$0) surface (bottom) exhibits two spin-orbit split Lorentzians originating from bulk (*b*) and surface (*s*) atoms, with a surface core-level

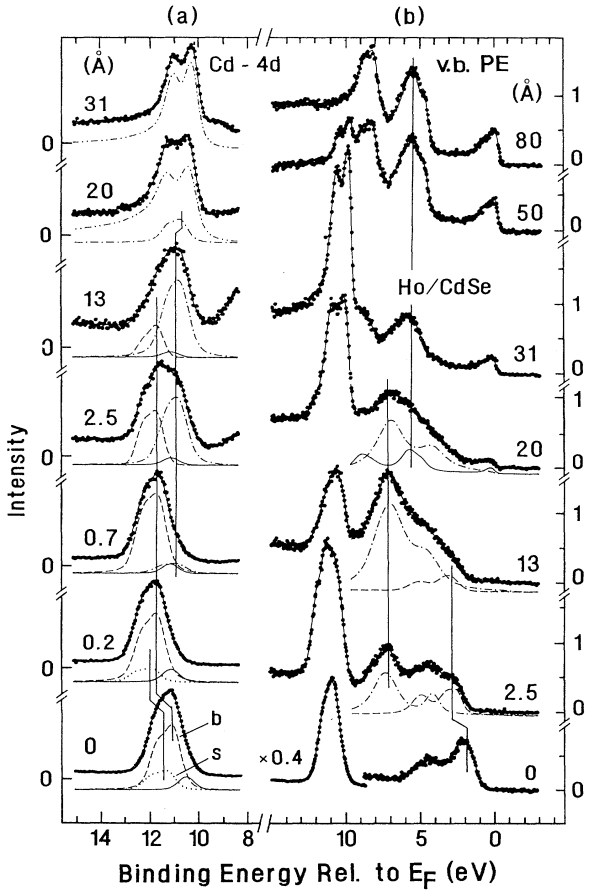

FIG. 1. PE spectra of the Ho/CdSe(10$\bar{1}$0) interface as a function of Ho coverage taken at $h\nu=50$ eV. (a) Cd 4*d* spectra; the solid lines through the data points represent the results of least-squares fits. The dashed subspectra stem from the unreacted bulk substrate, while the dash-dotted components originate from dissolved Cd. Dash-double-dotted curves represent signals from a metallic phase of Cd, while solid-line Lorentzians reflect the Se 4*s* intensity. Surface and bulk features are marked by *s* and *b*, respectively. (b) Overview valence-band PE spectra comprising the Ho 4*f* and Cd 4*d* BE regions together with the results of least-squares fits. The dashed subspectra represent the signal from the valence band of the unreacted CdSe substrate. The dash-dotted curves originate from the Ho 4*f* multiplet of the reacted Ho-Se phase, while solid subspectra stem from the valence band and 4*f* multiplet of metallic Ho.

shift of 0.25±0.05 eV and a spin-orbit splitting of 0.67±0.05 eV. The binding energy of the Cd $4d_{5/2}$ bulk component is found to be 11.02 eV. An additional Lorentzian peak at a BE of 10.35 eV simulates emission from Se 4*s* states (solid subspectrum). At a Ho coverage of $\simeq 0.2$ Å, all three components are simultaneously shifted by 0.58 eV to higher binding energies due to band bending. In addition, a decrease in the intensity of the surface component is observed, which is due to a quenching of the surface shift by Ho adatoms.

For Ho coverages of $\theta < 1$ Å, we observed only minor changes in the shape of the Cd 4*d* signal, pointing to a nonreactive interface. A new component (dash-dotted subspectrum), appearing at the low-binding-energy edge of the Cd 4*d* emission line, can be clearly identified for Ho coverages higher than this critical thickness of $\theta_c \simeq 1$ Å; it represents emission from a reacted phase. Upon further Ho deposition ($\theta \leq 13$ Å), the relative intensity of this dash-dotted component increases at the cost of the bulk signal from the substrate. The relatively broad (0.18 eV linewidth as compared to 0.13 eV for the unreacted phase) and structureless shape of this component indicates a rather inhomogeneous nature of the reacted phase. At coverages up to $\theta \simeq 13$ Å, the BE of this component does not change. For higher Ho coverages between 17 and 20 Å, an additional binding-energy shift of about 0.19 eV to lower values is observed, while the strongly reduced relative intensity of this reacted component complicates the BE analysis. Since this shift occurs when the valence-band spectrum reveals the appearance of a finite density of states at E_F [see Fig. 1(b)], we suggest that the origin of this shift lies mainly in an additional band bending due to metallization of the overlayer. This could then represent a transition from defect-induced Fermi-level pinning to a pinning caused by metal-induced gap states.[10]

Simultaneously with the metallization of the overlayer, drastic changes of the Cd 4*d* PE line shape are observed. For $\theta \geq 20$ Å, the spectra are characterized by a well-resolved asymmetric doublet as compared to the single-peaked structure at low Ho coverages. Such a spectral shape as well as the spin-orbit splitting of 0.83 eV for $\theta=31$ Å indicate the formation of a metallic phase of Cd.[15] Doniach-Sunjic line shapes[16] with an asymmetry parameter $\alpha=0.22$ were employed to fit this spectrum (dash-double-dotted line). The smeared-out doublet structure of the Cd 4*d* PE spectrum at $\theta=20$ Å can be explained by superposition of emissions from the reacted and the metallic Cd phases.

Figure 1(b) displays overview PE spectra taken at $h\nu=50$ eV comprising both the Cd 4*d* core-level and the valence-band PE regions. The spectra were normalized to constant photon flux in order to represent the intensity-versus-coverage dependence of the various spectral features. Note that the spectrum for the clean CdSe(10$\bar{1}$0) surface reveals the typical structure known for CdSe crystals,[17] while the one for high Ho coverages ($\theta \simeq 80$ Å) corresponds to the 4*f* (BE > 4 eV) and 5*d* (BE < 4 eV) spectral features characteristic for metallic Ho.[18] For a fit of valence-band spectra in the coverage range 2.5 Å $\leq \theta \leq$ 20 Å, a superposition of the line shapes

of clean CdSe ($\theta=0$ Å, dashed component) and thick Ho ($\theta=80$ Å, solid component) was used; both were allowed to adjust in amplitude and position. In addition, a component related to the reacted phase was necessary to fit the spectra, which was simulated by two Lorentzians (dash-dotted component) varying in position, width, and intensity with coverage.

In analogy to the Cd 4*d* PE lines, the valence-band structure of CdSe (bottom spectrum) is found to shift by 0.59 eV to higher binding energies for Ho coverages between 0 and 2.5 Å due to band bending (dashed subspectrum). Further Ho deposition up to $\theta=13$ Å leads to a suppression of the CdSe valence-band features and an enhancement of the Ho 4*f* multiplet structure (dash-dotted subspectrum). This 4*f* multiplet is broadened and shifted by $\simeq 1.33$ eV to lower binding energies as compared to that of metallic Ho, indicating the formation of an inhomogeneous reactive phase, which is caused by an interaction between Ho 5*d* and Se 4*sp* states. The remarkable difference observed in the spectral shapes and energy positions of the Se-*MVV* Auger signals for a clean CdSe surface and for Ho coverages higher than $\simeq 2$ Å supports this point of view (see inset in Fig. 2). The higher heats of formation of Ho selenides (−365 kJ/mol for HoSe and −962 kJ/mol for Ho_2Se_3) as compared to the heat of formation of CdSe (−163 kJ/mol) (Ref. 19) strongly favor the formation of Ho-Se compounds. Upon further Ho deposition, 13 Å $<\theta<$ 31 Å, the structure of the reacted Ho 4*f* component turns again sharper, exhibiting a 0.49-eV larger splitting of the two main Ho 4*f* features as compared to that for a coverage of $\theta=13$ Å. In addition, the characteristic 4*f*-multiplet structure of metallic Ho is obtained [solid subspectrum in Fig. 1(b)], which completely replaces the reacted component for Ho coverages of $\theta \geq 50$ Å.

In the Ho coverage range up to $\simeq 15$ Å, the integral Cd 4*d* PE intensity as well as the Cd 4*d* PE intensity from the substrate (bulk plus surface components) decrease gradually with increasing coverage [marked as Cd_{int} and Cd_{sub} in Fig. 2(b), respectively]. Then, for coverages between 20 and 30 Å, where surface metallization is observed, the Cd 4*d* PE intensity increases drastically, while a decrease in the PE signal from the Ho 4*f* states is observed. Additional Ho deposition ($\theta > 30$ Å) suppresses the PE signal from cadmium again. The sharp doublet structure of the Cd 4*d* PE spectrum, which can still be discerned in this coverage range, shows that Cd remains present in the metallic phase up to coverages of $\theta \simeq 50$ Å.

B. Auger attenuation curves and Auger depth-profile analysis

Information on the spatial distribution of Cd and Se released from the substrate is contained in the AES attenuation curves presented in Fig. 2(a). In the low-coverage regime, $\theta \leq 1$ Å, the attenuation of the Cd-*MNN* AES intensity (open squares) is remarkably faster than that of the Se-*MVV* AES intensity (open triangles). This fact as well as a gradual vanishing of the LEED pattern suggest an atomic rearrangement at the surface even before intense chemical reactions start. Upon further deposition of Ho, the Se-*MVV* AES intensity increases again due to interdiffusion and formation of a Ho-Se compound; this increase saturates at $\simeq 4$ Å, with approximately constant Se-*MVV* AES intensity up to $\simeq 15$ Å. At the same time, a decay of the Cd-*MNN* AES signal is observed. From the slopes of the attenuation curves for the Cd_{sub} 4*d* PE and the Cd-*MNN* AES signals, a value of $\simeq 4.5$ Å is obtained for the attenuation length in agreement with the expected electron-escape depth in the case of layer-by-layer growth. A huge peak of the Cd-*MNN* AES intensity in the coverage range 20 Å $<\theta<$ 40 Å, accompanied by a shallow dip in the Ho-*NON* AES signal intensity (open circles), reflects a new stage in the formation of the Ho/CdSe interface. At the same time, a considerable decrease in the Se-*MVV* AES intensity is observed. This behavior can be explained by either Cd

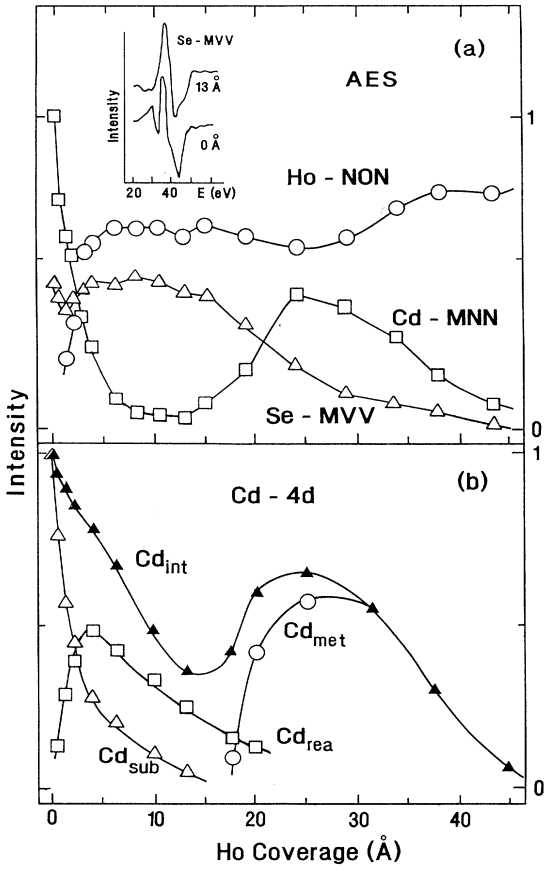

FIG. 2. Intensities of (a) the Cd-*MNN* (open squares), Se-*MVV* (open triangles), and Ho-*NON* (open circles) Auger signals and (b) the Cd 4*d* PE signals as a function of Ho coverage. For the PE intensities, filled triangles are used to denote the integral Cd 4*d* PE intensity (Cd_{int}), open triangles represent the signal from the substrate (Cd_{sub}), open squares mark the contribution from dissolved reacted Cd (Cd_{rea}), and open circles represent the signal from the metallic phase of Cd (Cd_{met}). The curves in (a) and (b) were normalized to the intensity of the Cd-*MNN* Auger or Cd 4*d* PE signals from a clean CdSe(10$\bar{1}$0) substrate, respectively. In the inset, Se-*MVV* Auger spectra from a clean CdSe(10$\bar{1}$0) surface as well as for a Ho coverage of $\theta=13$ Å are presented.

segregation or clustering of the reacted phase. In the following, we will further discuss these points. Even higher coverages by Ho result in a concurrent decay of both the Se and the Cd AES intensities and in a saturation of the Ho AES signal.

Analogous information on the formation of the Ho/CdSe interface is contained in the Cd 4*d* PE signal intensity presented in Fig. 2(b) as a function of Ho coverage. To allow a more detailed discussion, Fig. 2(b) contains the spectral intensities of the various components of the Cd 4*d* PE signal as a function of Ho coverage. The substrate component (Cd_{sub}, open triangles) decays rapidly and can no longer be observed for coverages higher than $\simeq 20$ Å. On the other hand, the integral Cd 4*d* PE intensity (Cd_{int}, filled triangles) shows a broad maximum at about 20–35 Å that correlates well with the huge peak in the Cd-*MNN* AES intensity; it is almost completely accounted for by the metallic Cd component (Cd_{met}, open circles). For intermediate Ho coverages, the Cd 4*d* PE intensity is mainly given by the reacted component (Cd_{rea}, open squares). Comparing the heats of formation of Ho selenides with that of CdSe,[19] we suppose that at these coverages Cd is rather dissolved in a reacted Ho-Se overlayer in analogy to the case of Al/CdSe(10$\bar{1}$0).[17]

Additional information on the spatial distribution of the elements in the interface layer was obtained by AES depth-profile analysis (see Fig. 3). Here, the AES signal intensities are plotted versus sputtering time for an interface of 30 Å of Ho deposited on CdSe(10$\bar{1}$0). Similar results have been obtained for other Ho coverages in the range 20 Å $< \theta <$ 40 Å. The initial maximum in the Cd-*MNN* intensity and the delayed onset in the Se-*MVV* intensity reflect the existence of a Cd-rich surface with only negligible amounts of Se, in good agreement with the conclusions from the PE and AES data. For longer sputtering times, the Cd AES intensity goes through a minimum. Simultaneously, the Se-*MVV* AES signal increases steeply, while the Ho-*NON* AES signal remains almost constant. In this depth (or sputtering-time) region, the reacted Ho-Se phase is monitored, with some Cd atoms dissolved. The following growth of the Cd-AES intensity together with the decrease in the Ho-AES intensity with increasing sputtering time shows that the CdSe substrate is reached by ablation through the sputtering process.

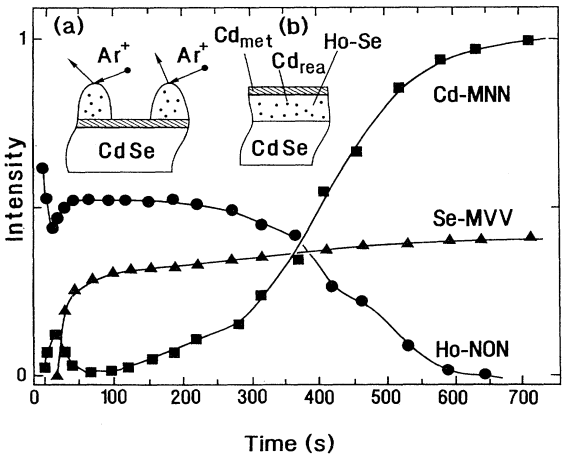

FIG. 3. Auger depth-profile intensities of Cd-*MNN* (filled squares), Se-*MVV* (filled triangles), and Ho-*NON* (filled circles) AES signals, normalized to the intensity of the Cd-*MNN* signal from the CdSe(10$\bar{1}$0) substrate, as a function of sputtering time for a 30-Å Ho/CdSe(10$\bar{1}$0) interface. The two insets show two structural models for the formation of the Ho/CdSe interface: (a) clustering of the reacted phase and (b) Cd segregation to the surface.

As mentioned above, the strong enhancements of the Cd 4*d* PE and Cd-*MNN* AES intensities observed for Ho coverages beyond $\simeq 20$ Å occur in parallel to a metallization of the overlayer. The question then remains if this is due to clustering of the reacted phase or due to Cd segregation to the surface. A clustering of the reacted phase [see inset (a) in Fig. 3] is unlikely, since this corresponds to the presence of a metallic Cd phase deep inside the junction, in disagreement with the results presented in Fig. 3. The results of AES depth-profile analysis using grazing-incident Ar^+ ions suggest the presence of a Cd-enriched surface, which strongly favors Cd segregation to the surface; this situation is schematically depicted by inset (b) in Fig. 3.

CONCLUSIONS

We arrive at the following picture for the interface formation between Ho and CdSe(10$\bar{1}$0): For Ho coverages smaller than a critical thickness of $\simeq 1$ Å, no significant reaction or intermixing of the components occurs. This conclusion, which is mainly based on the AES data, is not in contradiction to the weak intensity of a reacted component that can be distinguished in the fit analysis of the Cd 4*d* PE spectrum for a coverage of $\theta = 0.7$ Å [see Fig. 1(a)]. The occurrence of such a weak component can be explained by a lateral thickness variation of the deposited Ho layer.

The Cd 4*d* and valence-band PE spectra for $\theta \simeq 0.2$ Å reveal a shift to higher binding energies by $\simeq 0.58$ eV due to initial band bending. For coverages higher than a critical coverage of $\theta_c \simeq 1$ Å, strong interdiffusion of the components is observed, indicating an intense chemical reaction at the interface. This observation is analogous to the situation found previously for other reacted interfaces and correlates well with changes in the electronic structure of the overlayer when going from a more atomiclike to a solid-state configuration.[14]

We expect no reaction between Cd and Ho, since the formation of the only known Cd-Ho compound, with stoichiometry Cd_6Ho,[20] would require the breaking of six Cd-Se bonds per Ho atom. On the other hand, Cd-Se bonds can be broken by a Ho-Se reaction due to the substantial differences in the heats of formation of CdSe and Ho-Se compounds.[19] In spite of the relatively small heat of formation of HoSe (-365 kJ/mol) as compared to that of Ho_2Se_3 (-962 kJ/mol), the dilute concentration of Ho in the low-coverage regime favors a simple replacing of one Cd atom by one Ho atom, which leads to a release of only one Cd atom per Ho atom. We speculate that the Cd atoms remain then weakly bound within the HoSe domains intermixed with fragments of CdSe. In this

stage no Cd segregation would occur. Upon further deposition of Ho, neighboring Ho atoms can form the energetically preferred Ho_2Se_3 compound releasing three Cd atoms per two Ho atoms. A hint for the existence of such a process is given by the change in the shape of the Ho $4f$ subspectrum at a coverage, where surface metallization is observed [Fig. 1(b)]. An increase in the concentration of released Cd due to conversion of HoSe into Ho_2Se_3 would favor Cd segregation to the surface. Moreover, the growth of the interfacial layer will lead to an increase in the number of linear defects, which could serve as channels for Cd segregation. In this way, the Cd atoms will form a metallic overlayer leading to an increase in the density of electronic states at E_F. This surface layer of metallic Cd passivates the interface, favoring in the higher-coverage range the growth of a metallic Ho film on top of the interfacial layer.

ACKNOWLEDGMENTS

The authors thank Professor I. Broser, T. U. Berlin, for providing the CdSe single crystals used in this work. Expert experimental assistance by Dr. T. Ditzinger and by the staff of BESSY, in particular by Dr. W. Braun, is gratefully acknowledged. One of the authors (S.L.M.) thanks the Alexander von Humboldt Foundation and the Freie Universität Berlin, respectively, for financial support and hospitality. This work was supported by the Bundesminister für Forschung und Technologie, Project No. 05-5KEAXI-3/TP02.

*Permanent address: Institute of Physics, St. Petersburg State University, St. Petersburg 198904, Russia.

[1]L. J. Brillson, Surf. Sci. Rep. **2**, 123 (1982).

[2]L. C. Feldman and J. W. Mayer, *Fundamentals of Surface and Thin Film Analysis* (North-Holland, New York, 1986).

[3]J. Derrien, G. Le Lay, and F. Salvan, J. Phys. Lett. **39**, L287 (1978).

[4]M. Hanbücken and G. Le Lay, Surf. Sci. **168**, 122 (1986).

[5]A. Franciosi, J. H. Weaver, P. Perfetti, A. D. Katnani, and G. Margaritondo, Solid State Commun. **47**, 427 (1983).

[6]M. Grioni, J. Joyce, S. A. Chambers, D. G. O'Neill, M. del Giudice, and J. H. Weaver, Phys. Rev. Lett. **53**, 2331 (1984).

[7]J. Nogami, M. D. Williams, T. Kendelewicz, I. Lindau, and W. E. Spicer, J. Vac. Sci. Technol. A **4**, 808 (1986).

[8]J. J. Joyce, F. Boscherini, M. W. Ruckman, and J. H. Weaver, Phys. Rev. B **36**, 1605 (1987).

[9]B. M. Trafas, C. M. Aldao, C. Capasso, Y. Shapira, F. Boscherini, I. M. Vitomirov, and J. H. Weaver, Phys. Rev. B **40**, 9811 (1989).

[10]M. Prietsch, M. Domke, C. Laubschat, and G. Kaindl, Phys. Rev. Lett. **60**, 436 (1988).

[11]J. Onsgaard, J. Ghijsen, R. L. Johnson, M. Christiansen, F. Orskov, and P. J. Godowski, Phys. Rev. B **43**, 4216 (1991).

[12]V. K. Adamchuk, A. V. Fedorov, and S. I. Fedoseenko, Surf. Sci. **269/270**, 975 (1992).

[13]P. Singh and B. Baishya, Phys. Status Solidi A **104**, 885 (1987).

[14]S. L. Molodtsov, C. Laubschat, G. Kaindl, A. M. Shikin, and V. K. Adamchuk, Phys. Rev. B **44**, 8850 (1991).

[15]J. A. Nicholson, R. C. G. Leckey, J. D. Riley, J. G. Jenkin, and J. Liesegang, J. Phys. F **9**, 393 (1979).

[16]S. Doniach and M. Sunjic, J. Phys. C **3**, 285 (1970).

[17]C. F. Brucker and L. J. Brillson, J. Vac. Sci. Technol. **19**, 617 (1981).

[18]F. Gerken, J. Phys. F **13**, 703 (1983).

[19]*Gmelin: Handbook of Inorganic Chemistry: Sc, Y, La-Lu,* 8th ed. (Springer-Verlag, Berlin, 1986), Vol. C9; *Gmelin: Handbook of Inorganic Chemistry: Cd,* 8th ed. (Springer-Verlag, Berlin, 1975), Vol. 33.

[20]*Handbook of Lattice Spacings and Structures of Metals and Alloys 2,* edited by W. B. Pearson (Pergamon, New York, 1967), p. 185.